A Comparison of the Structural Response of Clamped and Simply Supported Sandwich Beams With Aluminium Faces and a Metal Foam Core

V. L. Tagarielli

N. A. Fleck
e-mail: naf1@eng.cam.ac.uk

Engineering Department,
University of Cambridge,
Trumpington Street,
Cambridge, CB2 1PZ, UK

Plastic collapse modes for clamped sandwich beams have been investigated experimentally and theoretically for the case of aluminium face sheets and a metal foam core. Three initial collapse mechanisms have been identified and explored with the aid of a collapse mechanism map. It is shown that the effect of clamped boundary conditions is to drive the deformation mechanism towards plastic stretching of the face sheets. Consequently, the ultimate strength and level of energy absorption of the sandwich beam are set by the face sheet ductility. Limit load analyses have been performed and simple analytical models have been developed in order to predict the postyield response of the sandwich beams; these predictions are validated by both experiments and finite elements simulations. It is shown experimentally that the ductility of aluminium face sheets is enhanced when the faces are bonded to a metal foam core. Finally, minimum weight configurations for clamped aluminium sandwich beams are obtained using the analytical formulas for sandwich strength, and the optimal designs are compared with those for sandwich beams with composite faces and a polymer foam core. [DOI: 10.1115/1.1875432]

1 Introduction

A large amount of research has been conducted recently on the mechanical performance of sandwich structures, stimulated by the development of stiff and strong, lightweight core materials [1–3]. For example, Chen et al. [4] and Bart-Smith et al. [5] have explored the quasi-static behavior of simply supported aluminium sandwich beams in three-point bending. The competing collapse modes of core shear, face yield, and indentation were observed, and the sensitivity of the collapse strength to geometry and to material properties was determined. However, there has been little prior attention paid to the effect of the support condition upon the collapse mechanism. Sandwich panels are often clamped to a stiff and strong support framework (e.g., a ship hull), and this can be represented in the laboratory by a fully clamped end condition.

In the present study, the response of sandwich beams comprising aluminium face sheets and an aluminium alloy foam core is explored for both simply supported and fully clamped boundary conditions. Potential modes of initial collapse are identified, and simple analytical models are stated. A mechanism map for initial collapse is generated from these formulas in order to relate the governing collapse mechanism of clamped beams to their geometry and material properties. Three sandwich geometries are selected from the collapse map, with each one lying in a different regime. Sandwich specimens with these geometries are manufactured and tested with both simply supported and clamped end conditions. The operative collapse mechanisms and measured load versus deflection curves are compared with both analytical predictions and finite element simulations. The analytical formulas for initial collapse are then used to determine minimum weight designs for clamped sandwich beams as a function of an appropriate structural load index. These minimum weight configurations are compared with minimum weight designs for clamped sandwich beams with composite face sheets and polymer foam cores. The study concludes with a short experimental study on the degree to which the foam core stabilizes the faces against necking.

Contributed by the Applied Mechanics Division of THE AMERICAN SOCIETY OF MECHANICAL ENGINEERS for publication in the ASME JOURNAL OF APPLIED MECHANICS. Manuscript received by the Applied Mechanics Division, March 5, 2004; final revision, September 18, 2004. Editor: R. M. McMeeking. Discussion on the paper should be addressed to the Editor, Professor Robert M. McMeeking, Journal of Applied Mechanics, Department of Mechanical and Environmental Engineering, University of California—Santa Barbara, Santa Barbara, CA 93106-5070, and will be accepted until four months after final publication in the paper itself in the ASME JOURNAL OF APPLIED MECHANICS.

2 Analytical Models for the Collapse Response

We begin by summarizing analytical formulas for the elastic stiffness, initial collapse load, and postyield behavior of sandwich beams, assuming that both face sheets and core can be considered as elastic—perfectly plastic materials, and the beams are either simply supported or fully clamped. The analytical formulas are used to construct collapse mechanism maps, and to enable the design of specimen geometries so that a variety of failure modes are activated.

Consider a sandwich beam of length ℓ and uniform width b, comprising two identical face-sheets of thickness t, bonded to a metal foam core of thickness c, as shown in Fig. 1. A flat-bottomed punch of width a is used to load the beam transversely at midspan by a force F and corresponding deflection u. The outer supports react with two vertical forces $F/2$ in the simply supported case plus bending moments M and in-plane horizontal forces P in the clamped case. When the beam is simply supported its length exceeds the span ℓ by an overhang H at each end.

A suffix f-denotes the face sheet, while the suffix c denotes the core; we introduce the symbols E_f, σ_f, ν_f, ρ_f, and E_c, σ_c, ν_c, ρ_c to denote the Young's modulus, yield strength, Poisson ratio, and density of the faces and core, respectively. It is useful to nondimensionalize the geometrical and material parameters according to the following definitions:

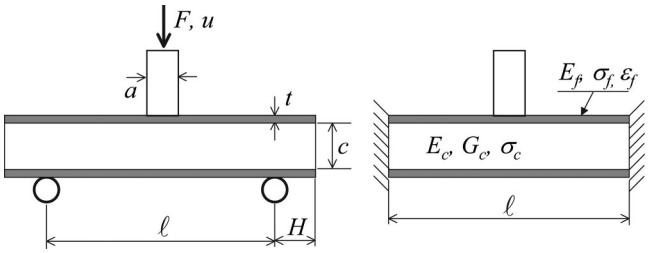

Fig. 1 Geometries of simply supported and clamped sandwich beams transversely loaded by a flat punch

$$\bar{c}=\frac{c}{\ell};\ \bar{t}=\frac{t}{c};\ \bar{a}=\frac{a}{\ell};\ \bar{u}=\frac{u}{\ell};\ \bar{\sigma}=\frac{\sigma_c}{\sigma_f};\ \bar{\rho}=\frac{\rho_c}{\rho_f} \tag{1}$$

Furthermore, we define the following nondimensional indices for the load F, energy absorption W, and mass M as:

$$\bar{F}=\frac{F}{b\ell\sigma_f};\ \bar{W}=\frac{W}{b\ell^2\sigma_f};\ \bar{M}=\frac{M}{b\ell^2\rho_f}=(2\bar{t}+\bar{\rho})\bar{c} \tag{2}$$

2.1 Elastic Regime. Elastic theory for sandwich beams is well established [6], and the transverse deflection u at midspan of the beam is

$$u=\frac{F\ell^3}{48EI_{\text{eq}}}+\frac{F\ell}{4AG_{\text{eq}}} \tag{3}$$

in the simply supported case, and

$$u=\frac{F\ell^3}{384EI_{\text{eq}}}+\frac{F\ell}{4AG_{\text{eq}}} \tag{4}$$

in the fully clamped case. The equivalent flexural and shear rigidities are given by

$$EI_{\text{eq}}=\frac{E_f btd^2}{2}+\frac{E_f bt^3}{6}+\frac{E_c bc^3}{12}\approx\frac{E_f btd^2}{2}$$
$$AG_{\text{eq}}=\frac{bd^2}{c}G_c\approx bcG_c \tag{5}$$

where G_c is the shear modulus of the core and $d=c+t$. The flexural and shear terms have comparable magnitudes for the sandwich beams considered later, and so it is necessary to include both.

2.2 Mechanisms of Initial Collapse. Consider the response of an elastic-ideally plastic sandwich beam, with an end condition of either fully clamped or simply supported. As the applied load is increased a limit load is attained, corresponding to initial plastic collapse. For the case of a clamped beam, membrane effects become significant with continued deformation beyond initial collapse, and a subsequent hardening behavior is observed.

The initial limit load for initial plastic collapse is calculated for a number of trial collapse mechanisms using the upper bound theory of plasticity. The face sheets and core are taken to be rigid, ideally plastic with uniaxial strength σ_f for the faces and σ_c for the core. Ashby et al. [1] have identified the competing collapse modes for sandwich beams with metallic face sheets and cores as *face yield*, *core shear*, and *indentation*. We calculate collapse loads for each of these mechanisms, for both simply supported and clamped boundary conditions, and since the transverse deflections are small, we neglect membrane effects.

In the current study only plastic collapse mechanisms are considered. Alternative failure modes are expected when the face sheets or core are made from elastic-brittle solids such as ceramics or ceramic-fiber composites.

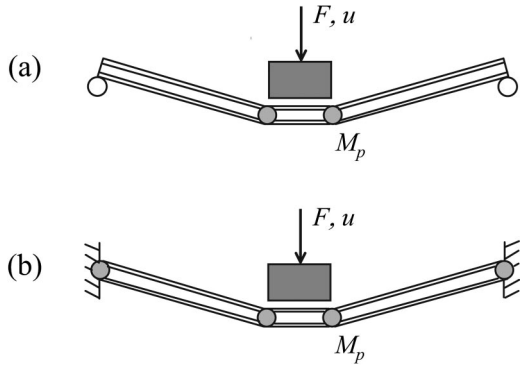

Fig. 2 Initial collapse by face yielding of sandwich beams (*a*) simply supported case and (*b*) built-in case

Face yield. Consider the plastic collapse of a simply supported sandwich beam, with the collapse mechanism given by rotation about plastic hinges adjacent to the central punch, as sketched in Fig. 2(*a*). The plastic bending moment for the beam is given by

$$M_p=dtb\sigma_f+\frac{c^2}{4}b\sigma_c \tag{6}$$

A straightforward work calculation gives the plastic limit load F_{FYS} for face yield of the simply supported beam as

$$F_{\text{FYS}}=\frac{4bt(c+t)}{\ell-a}\sigma_f+\frac{bc^2}{\ell-a}\sigma_c \tag{7}$$

which can be re-expressed in nondimensional form as

$$\bar{F}_{\text{FYS}}=\frac{F_{\text{FYS}}}{b\ell\sigma_f}=\frac{\bar{c}^2}{1-\bar{a}}[4\bar{t}(1+\bar{t})+\bar{\sigma}] \tag{8}$$

The same result can be obtained by considering equilibrium and yield, via the lower bound theorem, but this is not detailed here. Consequently, this formula is exact within the context of rigid, ideally plastic beam theory.

A closely related result follows for the clamped sandwich beam. Now, however, four plastic hinges exist, two at the punch and one at each support. The collapse load is twice that for the simply supported beam, and is given in nondimensional form as

$$\bar{F}_{\text{FYC}}=\frac{F_{\text{FYC}}}{b\ell\sigma_f}=\frac{2\bar{c}^2}{1-\bar{a}}[4\bar{t}(1+\bar{t})+\bar{\sigma}] \tag{9}$$

for face yield of the clamped beam.

Core shear. The transverse shear force on a sandwich beam is carried mainly by the core, and plastic collapse by core shear can result. Consider first the case of a simply supported sandwich beam with an overhang H beyond the outer rollers, as shown in Fig. 1. Two competing collapse mechanisms can be identified. Mode A entails plastic shear of the core and rotation about plastic hinges in the face sheets at the central punch, see Fig. 3(*a*), note that the sandwich beam shears beyond the outer supports. Alternatively, in mode B, the sandwich beam does not shear beyond the outer supports but this necessitates the formation of additional plastic hinges in the face sheets at the outer supports, see Fig. 3(*b*). Simple work calculations give the collapse loads for modes A and B, respectively, as

$$F_A=2\frac{bt^2}{\ell-a}\sigma_f+2bc\tau_c\left(1+\frac{H}{\ell-a}\right) \tag{10}$$

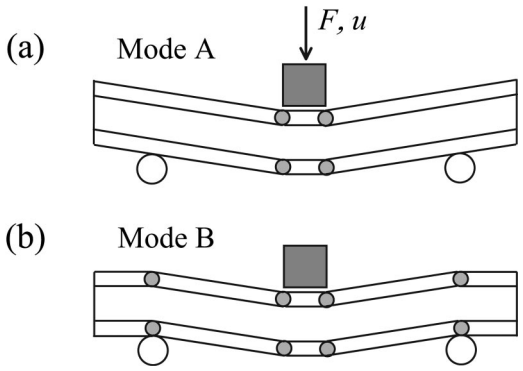

Fig. 3 Two alternative modes of initial collapse by core shear

$$F_B = 4\frac{bt^2}{\ell - a}\sigma_f + 2bc\tau_c \tag{11}$$

A comparison of these formulas confirms that mode A is more likely to occur at short overhangs; Chen et al. [4] have found the characteristic overhang H_t associated with transition from mode A to mode B

$$H_t = \frac{t^2\sigma_f}{2c\tau_c} \tag{12}$$

in which the shear strength of the core τ_c can be taken as $\tau_c \approx 2\sigma_c/3$.

For the case of clamped beams the only possible collapse mechanism is mode B, with the associated collapse load given by Eq. (11). In the present study we consider simply supported beams with an overhang length H exceeding the transition value H_t, so that the collapse mechanism is again mode B. The initial collapse load is insensitive to the boundary condition, and is given by the nondimensional form of (11), as

$$\overline{F}_{\rm CS} = \frac{F_B}{b\ell\sigma_f} = 4\overline{c}\left(\frac{\overline{ct}^2}{1-\overline{a}} + \frac{\overline{\sigma}}{3}\right) \tag{13}$$

Indentation. An alternative collapse mode is plastic indentation of the upper face sheet beneath the central punch, as sketched in Fig. 4. Again, a simple analytical formula can be obtained for the plastic collapse load using an upper bound approach, see Ashby et al. [1] and Bart-Smith et al. [5]. The mode involves plastic crushing of the core over a length of $(2\lambda + a)$ and the formation of four plastic hinges in the upper face sheet. The spacing λ between the hinges is obtained by minimizing the upper bound collapse load. For both the simply supported and clamped beams, the nondimensional indentation load is

$$\overline{F}_{\rm IN} = \frac{F_{\rm IN}}{b\ell\sigma_f} = 2\overline{tc}\sqrt{\overline{\sigma}} + \overline{a}\overline{\sigma}; \quad \lambda = t\sqrt{\frac{\sigma_f}{\sigma_c}} \tag{14}$$

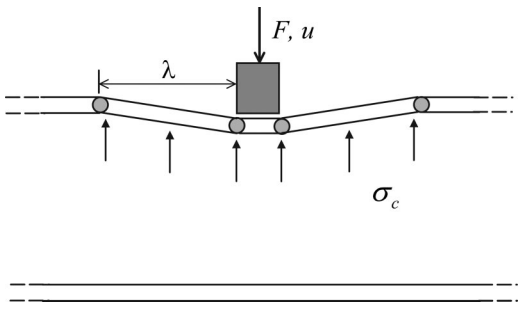

Fig. 4 Initial collapse of sandwich beams by indentation of the upper face sheet

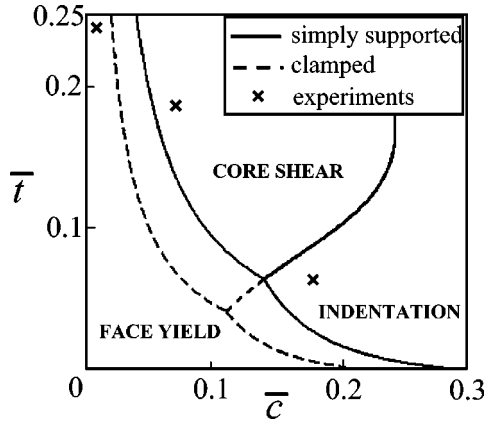

Fig. 5 Initial collapse mechanism map for simply supported and clamped sandwich beams in three-point bending. $\overline{\sigma}$ = 0.034 and $\overline{a}$ = 0.1. Test geometries are marked on the map.

2.3 Mechanism Maps for Initial Collapse. The observed initial collapse mechanism for a sandwich beam is the one associated with the lowest collapse load for a given geometry and material properties. The active modes can be shown graphically by plotting a nondimensional measure of the upper bound collapse load $\overline{F} = F/(b\ell\sigma_f)$ on a diagram with the nondimensional axes $\overline{c}$ and $\overline{t}$, for selected values of $\overline{\sigma}$ and $\overline{a}$. This method follows that pioneered by Gibson and Ashby [7] for polymeric foam cores and aluminium alloy face sheets.

A collapse mechanism map, for both simply supported and clamped beams, is given in Fig. 5, for the choice $\overline{\sigma} = 0.034$ and $\overline{a} = 0.1$, and the map is representative of the materials used in this study. It is assumed that the overhang H for the simply supported case exceeds the transition value H_t so that core shear mechanism is mode B. The regimes of dominance for each collapse mechanism are marked, and the three data points marked on the figure give the three structural geometries tested and analyzed later.

Note that the maps for simply supported and fully clamped coincide along the indentation—core shear boundary, since only the face yield collapse load changes when we switch from the simply supported to the clamped boundary condition. The regime of face yielding is significantly larger for the simply supported beam than for the fully clamped beam.

2.4 Finite Deflection of Clamped Sandwich Beams. It is shown experimentally and theoretically later that simply supported beams undergo continued plastic collapse at nearly constant load; eventually, the transverse deflection becomes sufficiently large that the structure fails by fracture of the face sheets or core. In contrast, clamped beams undergo membrane stretching of the face sheets beyond initial yield, and this gives rise to a hardening macroscopic response. We now analyze the postyield response of clamped sandwich beams.

Initial plastic collapse of clamped sandwich beams occurs by face yield, core shear, or indentation at small transverse deflections. Subsequent transverse deflection, however, involves tensile stretching of the faces and core. The stress distribution within the beam evolves from that associated with the initial collapse load to that of pure membrane action, with the membrane solution achieved when the deflection is about equal to the thickness of the beam $H_S = C + 2t$. Thereafter, the beam deforms in a membrane mode, and yields axially until the face sheets tear when the axial plastic strain attains the material ductility. Equilibrium considerations give an expression for the load versus deflection response in the membrane phase as

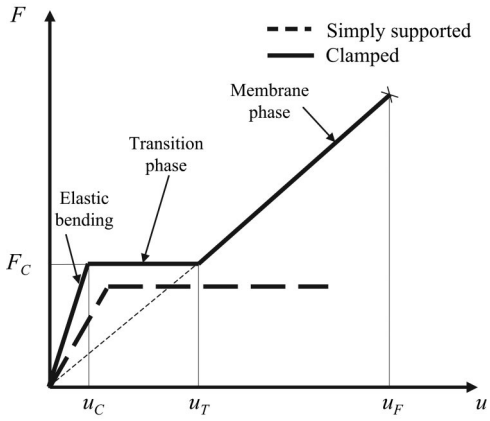

Fig. 6 Stages of collapse of simply supported and clamped sandwich beams

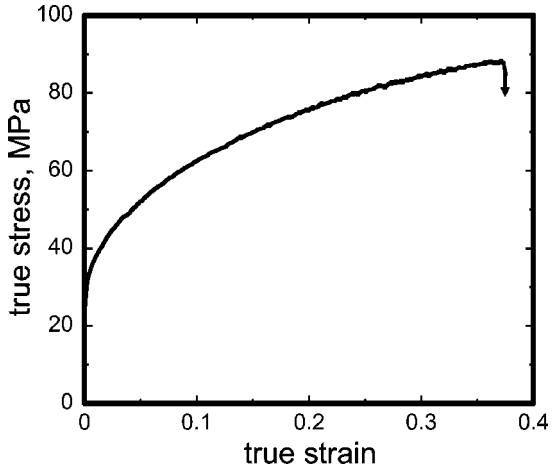

Fig. 7 Tensile response of the annealed aluminium face sheets

$$F(u) = \frac{8tb\sigma_f}{\ell - a}u \tag{15}$$

assuming that the deflection u is small compared with the span ℓ, and that the net axial force in the faces is much greater than that in the core.

It is difficult to obtain a general failure criterion for the beam, since the plastic strain distribution within the sandwich structure depends upon both the initial collapse mechanism and the membrane stretching phase of deformation. Here, we state a simple failure criterion based on an estimate of the strain in the face sheets due to stretching of the beam, and neglect the plastic strains due to bending. For an assumed ductility ε_F of the face sheet material, the deflection u_F at failure is given by

$$u_F = \ell\sqrt{\tfrac{1}{2}(1-\bar{a})\varepsilon_F} \tag{16}$$

2.5 Summary of Clamped Beam Response. The load versus deflection response of clamped beams may be subdivided into three phases, as sketched in Fig. 6

(1) *Elastic bending*. The beam deflects elastically until the applied load attains the initial collapse load F_C associated with the operative collapse mechanism. The load F_C is reached at an elastic deflection u_C as dictated by Eq. (4).
(2) *Plateau phase*. Once initial collapse has been attained, it is assumed that the load remains constant under increasing transverse deflection up to a transverse deflection u_T, at which the load predicted by (15) equals the initial collapse load.
(3) *Membrane phase*. The beam stretches in the manner of a plastic string and the load versus deflection response is given by Eq. (15). The sandwich beam deflects until there is a sudden loss of load carrying capacity due to face sheet tearing when the deflection attains the value u_F.

The energy absorption W is the area under the load versus deflection curve of the sandwich beam. Upon neglecting the elastic contribution to energy absorption, the nondimensional measure $\bar{W} = W/b\ell^2\sigma_f$ for a clamped beam, is taken as

$$\bar{W} = \bar{F}_c\bar{u}_T + \frac{4\bar{t}\bar{c}}{1-\bar{a}}(\bar{u}_F^2 - \bar{u}_T^2) \tag{17}$$

where

$$\bar{u}_T = \frac{u_T}{\ell}; \quad \bar{u}_F = \frac{u_F}{\ell} \tag{18}$$

3 Materials Characterization and Test Technique

Three structural geometries have been selected within the failure map of Fig. 5, with each geometry lying in a different region of the map. The sandwich beams (of width about 50 mm) were manufactured by bonding aluminium face sheets to aluminium alloy foam cores, and were subsequently tested in three-point bending. A commercially pure fully annealed aluminium sheet was used to manufacture the faces, whereas the foam core was a closed-cell aluminium-alloy foam, with trade-name Alporas[1]; its relative density (density of the foam divided by the density of the cell wall material) was $\hat{\rho}=11\%$, and the average cell size was 3 mm. Annealed aluminium was used to ensure that the clamped specimens did not fail in the transition phase, in order to observe the membrane regime.

The aluminium face sheets were degreased and abraded, and were then adhered to the foam core using Redux 322 epoxy adhesive on a nylon carrier mesh. The sandwich beams were air-cured at 180 °C for 1 h, and bonding was facilitated by imposing a dead load with a nominal contact pressure of 0.01 MPa. The shear strength of the cured Redux 322 adhesive was taken to be 20 MPa, from Hexcel's data sheets: this strength is about one order of magnitude higher than that of the Alporas foam, and so no adhesive failure was observed.

3.1 Face Sheet Material. The mechanical properties of the annealed aluminium face sheets material were measured as follows. Tensile specimens of dog-bone geometry were cut from the aluminium face sheets. The tensile tests were performed in a servo hydraulic test machine at a strain rate of 10-4/s; the axial strain was measured using both strain gauges and a laser extensometer, while the transverse strain was measured with a strain gauge.

The measured true stress versus true strain response is given in Fig. 7. The Young's modulus is $E_f=70$ GPa, and the Poisson ratio is $\nu_f=0.33$. The annealed aluminium has a 0.2% offset yield strength of 30 MPa, an ultimate tensile strength of 85 MPa and an elongation to failure of about 40%.

3.2 Core Material. The tensile, compressive, and shear stress versus strain response has been already reported by Chen et al. [4]. In brief, the Young's modulus of the Alporas foam is $E_c=1.06$ GPa, and the compressive and tensile yield strength is $\sigma_c=2.1$ MPa, with a tensile ductility of 1.1%.

3.3 Test Method for Sandwich Beams. The sandwich beams

[1]European supplier, Karl Bula, Innovation Services, Ch-5200 Brugg, Herrenmatt 7F, Switzerland.

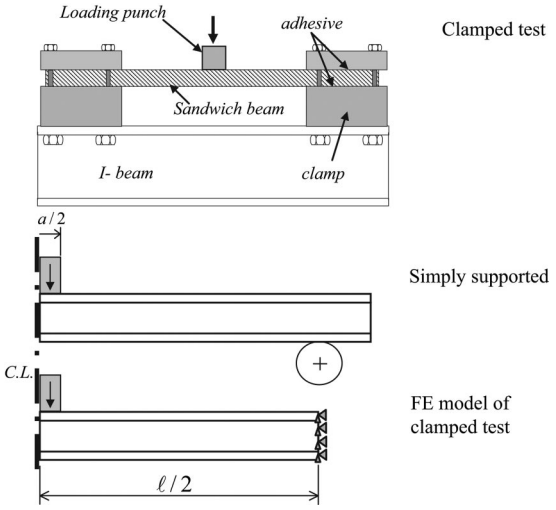

Fig. 8 The loading configurations, with boundary conditions used in the finite element calculations

were loaded in three point bending using a fully clamped rig and a simply supported rig, as sketched in Fig. 8. Selected specimens were instrumented in order to confirm the mechanism of collapse. Laser extensometers were used to measure the deflection and the change in height of beam directly under the indenter, and 120Ω resistance strain gauges of length 2 mm were placed at midspan on the bottom face sheet. A clip gauge was used to measure the relative sliding displacement of the face sheets, and thereby the average shear strain in the core.

The sandwich beams were loaded at a constant speed of 0.3 mm/s by flat indenters of width 0 (roller) to 18 mm. Fixed rollers of diameter 19 mm were used in the simply supported tests, while a stiff steel rig, bolted to an underlying I-beam, was used in the fully clamped tests to restrain the specimens against end displacement and rotation.

4 Effect of Boundary Conditions on Collapse Response

In order to investigate the effect of boundary conditions on the response of sandwich beams, three geometries of specimen have been manufactured and tested in the simply supported and clamped conditions. The geometries are summarised in Table 1. For each geometry, we compare the measured load versus deflection response of the clamped and simply supported beams.

4.1 Face Yield Specimens. Consider first the measured collapse response of beams undergoing face yield, see Fig. 9(*a*). The two beams initially collapse at different load levels; as predicted by Eqs. (8) and (9), the collapse load for the clamped beam is about twice that for the simply supported beam. After initial collapse, the simply supported beam deflects at almost constant load; it fails by tearing of the bottom face at midspan when the tensile plastic strain has attained the material ductility. The clamped beam first undergoes face yield; then, at deflections exceeding the thickness of the sandwich beam, the deformation mode switches to plastic stretching of the faces and core. This stretching phase is characterized by a steeply rising linear load versus deflection response. Both the simply supported and clamped tests were arrested prior to tensile tearing of the face sheets. Figure 9(*a*) includes photographs of two duplicate specimens tested under different boundary conditions. The extent of deflection of these duplicate specimens is labeled on the collapse responses. The two different modes of collapse at large deflections are evident.

Table 1 Geometry of sandwich beam specimens

No.	t(mm)	c(mm)	l(mm)	a(mm)
1 (FY)	0.8	3	200	0 (roller)
2 (CS)	0.8	4	70	18
3 (IN)	0.8	15	100	3.5

4.2 Core Shear Specimens. Figure 9(*b*) gives results for the sandwich beams initially collapsing by core shear. Again, the tests were not taken to final failure and again photographs are shown of two duplicate specimens. The degree of deflection of these duplicate specimens is labeled on the load versus deflection curves to aid their interpretation.

The simply supported beam was given a very large overhang in order to inhibit collapse by core shear mode A. With this choice, the initial collapse mechanism (and therefore the initial collapse load) is identical for the clamped and simply supported cases. The measured responses confirm this prediction, see Fig. 9(*b*). Now consider the collapse responses beyond initial yield. The load carried by the simply supported beam increases slightly to a peak value at a large transverse deflection of 8 mm. The peak in the load versus deflection curve is due to shear fracture of the foam core.

In contrast, the clamped beam undergoes axial stretching of the faces beyond initial collapse and the load steeply rises above the initial collapse strength, as suggested by Eq. (15). After a transition phase, of up to $u \approx H_S$, the load rises almost linearly with deflection; this supports the assertion of the analytical model that the specimen is in a pure membrane state.

Visual observations during the tests on the clamped and simply supported beams revealed that inclined shear cracks developed within the core once the core had sheared by a few percent. This is consistent with the fact that the Alporas foam has a shear ductility of 2%, see Chen et al. [4].

4.3 Indentation Specimens. The load versus deflection responses of the indentation geometry are given in Fig. 9(*c*), together with photographs of the as-tested specimens. It is clear from the images that the specimens are squat in shape and collapsed by indentation. Visual observations during each test confirmed that initial collapse was by indentation beneath the central punch. The initial collapse load of the clamped beam is approximately 20% greater than that of the simply supported beam, while the analytical predictions for the rigid, ideally plastic case give an identical yield load for both grip conditions. A possible explanation is that the bending moment at midspan for the clamped case is only half that for the simply supported case, at any given load. Therefore, the higher bending moments in the simply supported beam give rise to higher compressive stresses within the upper face sheet, and this facilitates the indentation mechanism.

Now consider the finite collapse response of the beams subsequent to the initial collapse. For the simply supported specimen, the separation of the faces diminishes with increasing transverse deflection, and so the plastic collapse moment (and consequently the applied load) drops. Finally, the bottom face tears at midspan.

In the clamped beam test the continued activation of the indentation mechanism is inhibited by the development of membrane tension within the faces. At sufficiently large transverse deflections the stress state again approaches the pure membrane state.

Figure 9(*c*) includes photographs of the as-tested specimens. Although the total transverse deflection is very similar in the two specimens, the degree of core crushing in the clamped beam is much less than that observed in the simply supported beam. This is consistent with the fact that tensile membrane stresses within the indented face of the fully clamped specimen have stabilized it against indentation.

5 Numerical Simulation of Beams Response

The three-point bending response of simply supported and clamped sandwich beams has been modelled with the commercial

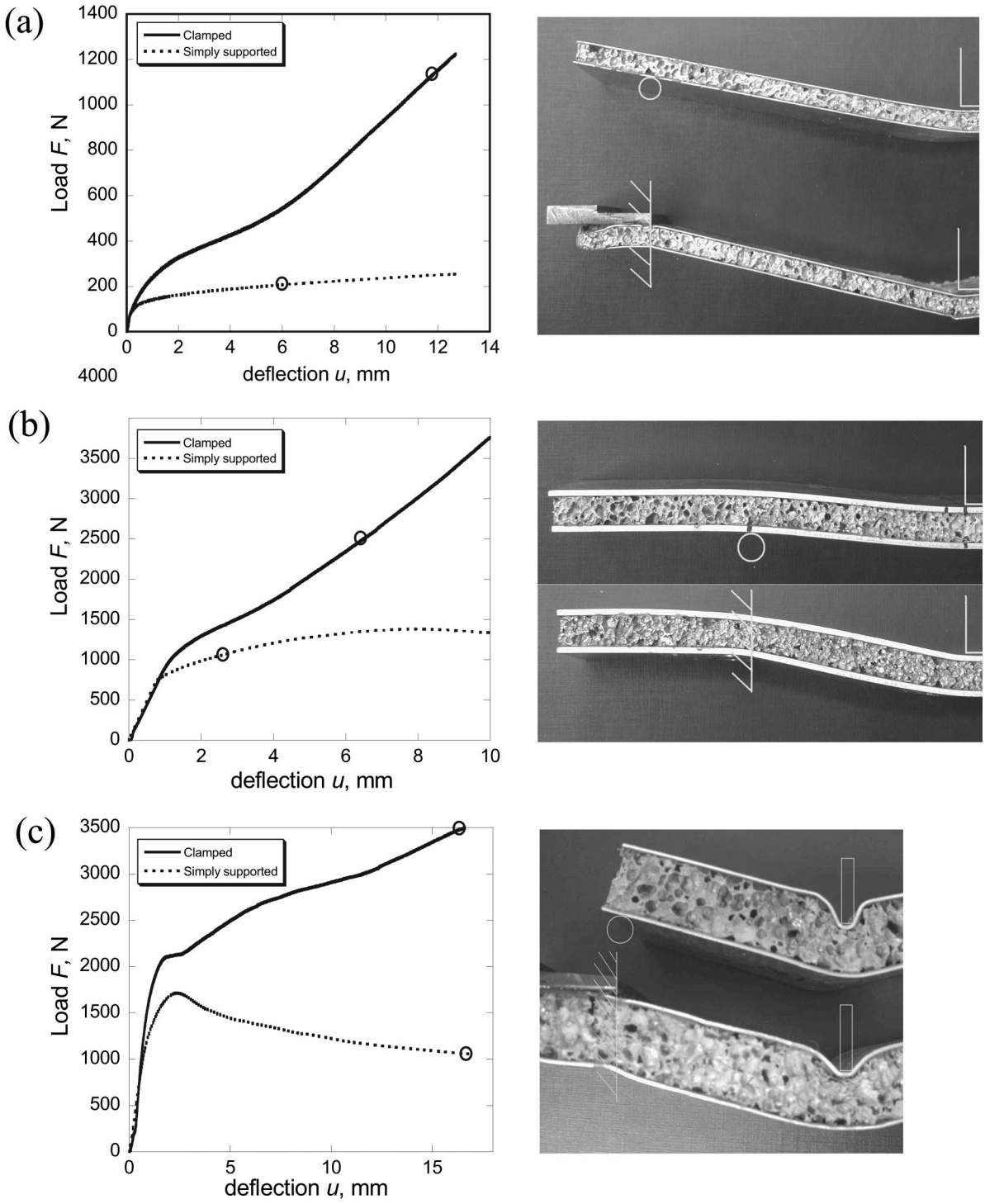

Fig. 9 Measured load vs deflection response and photographs of simply supported and clamped sandwich beams. Initial collapse is by (*a*) face yield, (*b*) core shear, and (*c*) indentation

finite elements code ABAQUS in order to compare it with analytical predictions and experiments. Due to symmetry, only half the length of the sandwich structure has been modeled. Eight-noded two-dimensional rectangular elements, with full integration, have been used to discretize the sandwich core and the aluminium skins. Typically, each face sheet has three elements in the thickness direction and 200 elements along the semi-span, while the core is twenty elements deep by 200 elements along the semi-span.

Loading by the frictionless flat punch is modeled by prescribing a uniform vertical displacement to the appropriate boundary nodes of the upper face sheet, as sketched in Fig. 8. In the simply supported case, contact between the beam and the rollers is modeled by the contact surfaces provided by ABAQUS. In the clamped case, both the vertical and horizontal displacements of nodes along the ends of the beam are constrained to vanish. This boundary condition is somewhat stiffer than the actual clamped condition used in the experimental investigation, see Fig. 8. A preliminary mesh sensitivity study has been performed to ensure an accurate representation of the sandwich specimen.

In the finite element model, the aluminium skins are modeled by the J_2 flow theory of plasticity, and the foam is described by the metal foam constitutive model of Deshpande and Fleck [8], as implemented in ABAQUS by Chen [9]. In this model the yield function Φ is assumed to be

$$\Phi = \hat{\sigma} - Y = 0 \tag{19}$$

where Y is the uniaxial yield strength and $\hat{\sigma}$ is the effective stress, defined by

$$\hat{\sigma}^2 = \frac{1}{1+(\alpha/3)^2}(\sigma_e^2 + \alpha^2\sigma_m^2) \tag{20}$$

where α defines the aspect ratio of the elliptical yield surface in the Mises stress σ_e and mean stress σ_m space. For the case $\alpha=0$, the effective stress $\hat{\sigma}$ reduces to σ_e and the J_2 flow theory is recovered. For simplicity, isotropic hardening is assumed, i.e., the yield surface grows in a geometrically self-similar manner with strain. To model the postyield behavior, an effective plastic strain rate $\dot{\hat{\varepsilon}}$, the work rate conjugate to $\hat{\sigma}$, is introduced as

$$\dot{\hat{\varepsilon}}^2 = [1+(\alpha/3)^2](\dot{\varepsilon}_e^2 + \dot{\varepsilon}_m^2/\alpha^2)$$

$$\dot{\varepsilon}_e^2 = (2/3)\dot{\varepsilon}_{ij}^p\dot{\varepsilon}_{ij}^p, \quad \dot{\varepsilon}_m = \dot{\varepsilon}_{ii}^p \tag{21}$$

where $\dot{\varepsilon}_{ij}^p$ is the plastic strain rate, $i,j=1,2,3$, and the convention of summation over repeated indices applies. With the assumption of normality, the plastic strain rate is given by

$$\dot{\varepsilon}_{ij}^p = \dot{\hat{\varepsilon}}\frac{\partial\Phi}{\partial\sigma_{ij}} = \frac{\dot{\hat{\varepsilon}}}{1+(\alpha/3)^2}\left(\frac{3}{2}\frac{s_{ij}}{\hat{\sigma}} + \frac{\alpha^2}{3}\delta_{ij}\frac{\sigma_m}{\hat{\sigma}}\right) \tag{22}$$

where $s_{ij}=\sigma_{ij}-\sigma_m\delta_{ij}$ is the deviatoric stress, δ_{ij} is the Kronecker delta, and the effective strain rate is connected to the effective stress rate by

$$\dot{\hat{\varepsilon}} = \frac{\dot{\hat{\sigma}}}{H(\hat{\sigma})} \tag{23}$$

Here, $H(\hat{\sigma})$ is the tangent of the uniaxial true stress versus logarithmic plastic strain curve at stress level $\sigma=\hat{\sigma}$. The constitutive models for both the aluminium faces and the foam core were calibrated against measured uniaxial data.

6 Comparison of Experiments and Predictions

It is instructive to compare the analytical predictions of the elastic-plastic collapse response with detailed finite element analysis for the three clamped beam geometries as detailed in Table 1 and shown in Fig. 5. A similar comparison has already been presented by Chen et al. [4] for simply supported aluminium sandwich beams, where excellent agreement is demonstrated.

Figure 10 shows the measured and predicted load versus deflection response for a specimen initially collapsing by face yield, core shear, and indentation, respectively. Each plot includes the analytical predictions of the elastic stiffness, the initial collapse load and the large-deflection membrane solution. The predicted transition point between the end of initial plastic collapse and the start of the membrane phase occurs at a deflection equal to the height of the beam, and this transition point is marked in the figures.

It is clear from Figs. 10(*a*) and 10(*b*) that, for the cases of face yield and core shear, there is a good agreement between the analytical predictions, the numerical model and the measured response. In particular, the prediction of the membrane phase accurately captures the measured response at $u>H_S$. In contrast, both the finite element predictions and analytical formulas underestimate the measured initial collapse load for the specimen collapsing by indentation, see Fig. 10(*c*) It is argued that this is due to the fact that the predictions neglect the presence of a strengthened boundary layer within the metal foam. This phenomenon has been

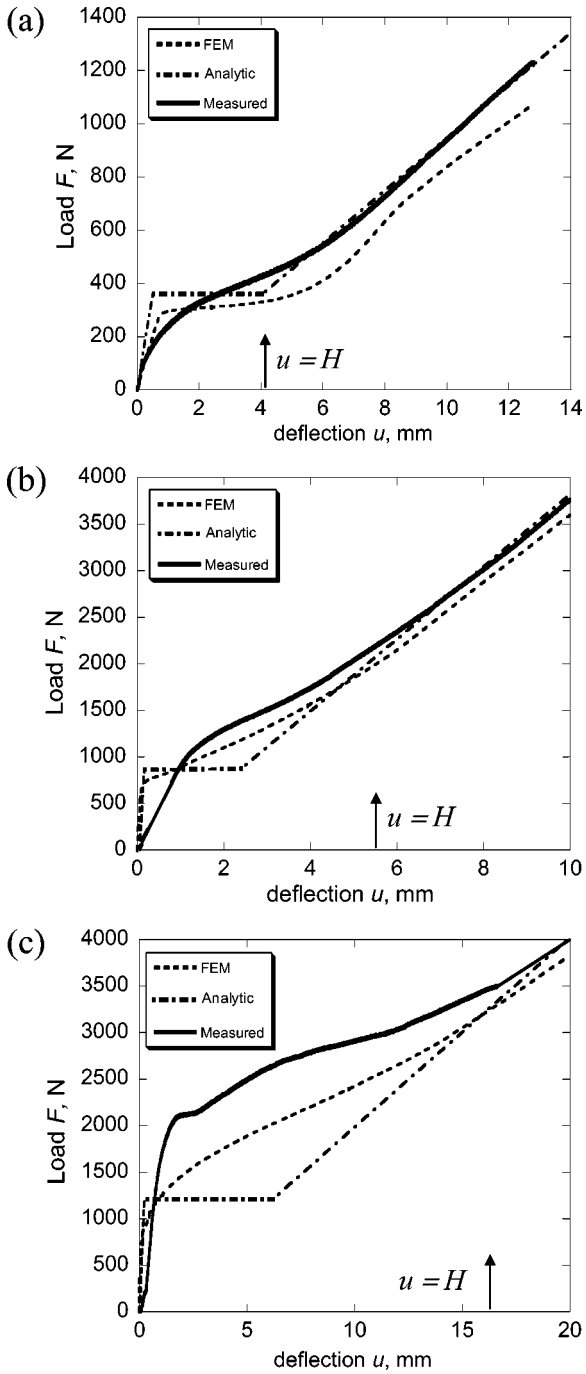

Fig. 10 Comparison of measured and predicted collapse responses for sandwich beams collapsing by (*a*) face yield, (*b*) core shear, and (*c*) indentation

observed previously for simply supported beams by Chen et al. [4], and has been analyzed in detail by Chen and Fleck [10]. They have discussed boundary layers for sandwich layers subjected to simple shear and shown experimentally and theoretically that the strength is enhanced when the thickness of the core is comparable to the cell size. A similar elevation is expected when the width of the indenter is comparable to the cell size, as in the present study. The source of the boundary layer is the fact that the foam cell walls are adhered to the face sheets and behave as encaster beams. For the indentation geometry the membrane solution is recovered when the transverse deflection u is comparable to the height H_S of the sandwich beam; the predicted large deflection solutions are again in reasonable agreement with the measured response.

Table 2 Geometry, face sheet strength, and observed mechanism of initial collapse for an additional set of experiments (key: SS = simply supported, CL = clamped, FY = face yield, CS = core shear, IN = indentation)

Spec. No.	t(mm)	c(mm)	l(mm)	a(mm)	b(mm)	Face sheet alloy	σ_Y(MPa)	Support conditions	Observed collapse mode
1	0.5	7	240	19	56	1	110	SS	FY
2	0.5	7	240	19	56	1	110	CL	FY
3	2	10	160	12.6	49	2	287	SS	CS
4	2	10	160	12.6	49	2	287	CL	CS
5	0.5	40	160	12.6	50	3	90	SS	IN
6	0.5	40	160	12.6	50	3	90	CL	IN
7	3	19	220	19	57	1	120	CL	CS
8	2	10	160	12.6	49	2	287	CL	CS
9	0.5	7	100	8	50	3	90	CL	CS
10	0.5	40	160	12.6	50	3	90	SS	IN
11	0.5	42	220	19	57	4	70	SS	FY
12	3	19	220	19	57	1	120	SS	CS
13	0.5	42	220	19	57	4	70	CL	FY

Additional Tests. Additional tests have been performed on clamped and simply supported specimens, using Alporas foam core and four different grades of aluminium alloy for the face sheets (the alloys are labeled in Table 2 as alloy 1 =BS HH/S1C, alloy 2=BS HE30TF, alloy 3=BS HH/S1C, and alloy 4=commercially pure, fully annealed aluminium). The geometry and strength of the faces have been varied over a wide range in order to explore the accuracy of the analytical predictions of initial collapse strength. A summary of the specimen geometries and the associated face sheet properties is presented in Table 2. The predicted mode of collapse is in agreement with the observed mode. In Fig. 11 the predicted initial collapse loads are compared with the corresponding measured values. It is evident that the analytical predictions are adequate for design purposes.

7 Minimum Mass Design of Clamped Sandwich Structures

A common requirement is to optimize the design to achieve a minimum mass for a given structural stiffness, strength, or level of energy absorption. Here we make use of the formulas developed in Sec. 2 in order to design clamped sandwich beams of minimum mass for a given initial collapse strength in three point bending. A complementary optimisation task has already been performed for simply supported aluminium sandwich beams by Chen et al. [4].

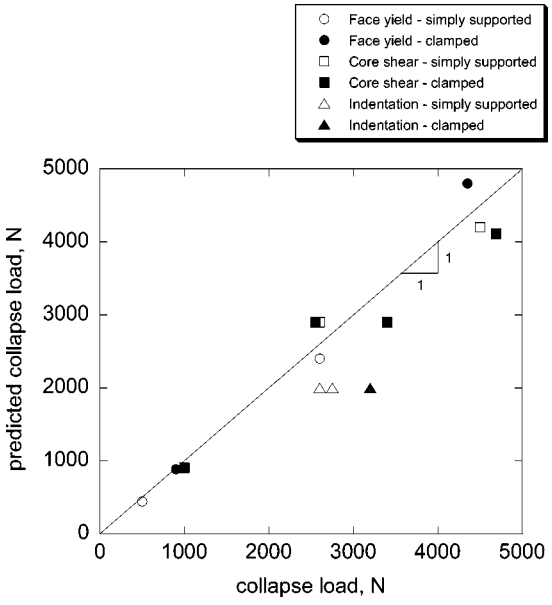

Fig. 11 Comparison of measure and analytical prediction of initial collapse strength for the specimens listed in Table 2

The first step is to construct a collapse mechanism map in terms of the nondimensional geometrical parameters $\bar{c}=c/\ell$ and $\bar{t}=t/c$, for a given a set of material properties of face sheets and core. A typical map is given in Fig. 12 for a clamped sandwich beam with aluminium alloy faces and an Alporas foam core, with the choice $\bar{\sigma}=\sigma_c/\sigma_f=0.034$, $\bar{a}=a/\ell=0.1$, $\bar{\rho}=0.11$. The dominant collapse modes are shown, as in Fig. 5, along with contours of nondimensional collapse load $\bar{F}=F/b\ell\sigma_f$ and mass $\bar{M}=M/b\ell^2\rho_f$. The geometry which minimises $\bar{M}$ at any fixed $\bar{F}$ is obtained by scanning along the contour of $\bar{F}$ to locate the point where the gradient $\nabla\bar{M}$ is locally parallel to $\nabla\bar{F}$. Upon repeating this procedure for increasing values of $\bar{F}$ a minimum mass trajectory is located, as shown in Fig. 12. Algebraic calculations, not reported here for the sake of brevity, give explicit analytical expressions for the dependence on the minimum mass index $\bar{M}_{\min}$ as a function of the required structural strength $\bar{F}$.

The definitions (2) for $\bar{F}$ and $\bar{M}$ involve the strength σ_f and density ρ_f of the face sheets. To allow for a direct comparison of the performance of various material combinations, the normalized values $\bar{F}^N$ of $\bar{F}$ and $\bar{M}^N$ of $\bar{M}$ are introduced, by using the strength σ_s and density ρ_s of a medium strength steel, taken as 400 MPa and 8000 kg/m^3, respectively;

$$\bar{F}^N=\frac{\sigma_f}{\sigma_s}\bar{F};\quad \bar{M}^N=\frac{\rho_f}{\rho_s}\bar{M} \tag{24}$$

The normalized minimum mass design $\bar{M}^N_{\min}$ is plotted as a function of the structural load index $\bar{F}^N$ in Fig. 13. The figure includes

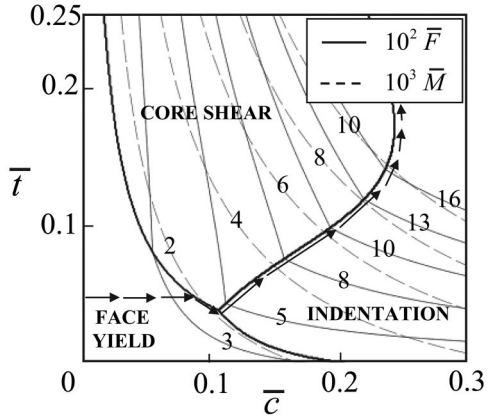

Fig. 12 Collapse mechanism map with contours of the nondimensional strength and mass index ($\bar{\sigma}=0.034, \bar{a}=0.1, \bar{\rho}=0.11$). The minimum mass trajectory is included.

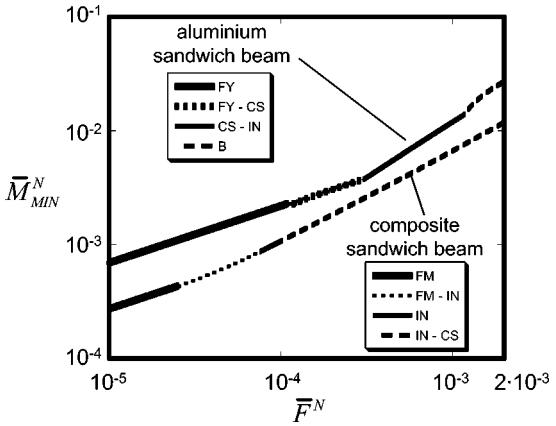

Fig. 13 Normalized minimum mass vs structural load index for a clamped sandwich beam of metallic construction and of composite construction (key: FM = face microbuckling, FY = face yield, CS = core shear, IN = indentation)

the minimum weight design plot for a clamped beam with glass-vinylester composite faces and H100 Divinycell foam core, taken from a parallel study [11]. The metallic sandwich performance is similar to that of the composite construction, and additional benefit would accrue from the use of heat-treated aluminium alloy face sheets.

8 Effect of Foam Core Upon Plane Strain Necking of Face Sheets

The present experimental study made use of annealed aluminium alloy face sheets. These possessed adequate strain hardening capacity to maintain stability and not undergo necking during the beam bending tests. Preliminary experiments (not reported here) using high strength aluminium alloy revealed that the peak load of clamped beams is set by sheet necking of the faces.

It is anticipated that the presence of a foam core delays the onset of tensile necking of the face sheets in the membrane phase of the response. Sheet metal necking involves a local reduction in thickness of the sheet, and a foam core provides resistance to this instability. This phenomenon has been explored experimentally as follows. Dog-bone shaped tensile specimens were made from a sandwich plate with faces comprising a BS HH/S1C grade of commercially pure, cold rolled aluminium of thickness t =0.9 mm, and Alporas form core of relative density 11% and thickness in the range 3–25 mm. The dog-bone specimens had a gauge length of 70 mm and a width of 25 mm; testing of the sandwich specimens was performed both along the rolling direction of the faces and transverse to the rolling direction.

The choice of material for the face sheets of the sandwich specimens was dictated by the requirement for the faces to undergo tensile necking at a low ductility (of the order of 1%) prior to tensile rupture of the foam core. The measured tensile ductility of the faces was ε_F=0.82% in the rolling direction and ε_F =1.12% in the transverse direction; for the two orientations the 0.2% offset yield strength equals 100 and 120 MPa, respectively.

Longitudinal sections of the necked face sheet are shown in Fig. 14(*a*) (no foam core present) and in Fig. 14(*b*) (foam core present). A typical load versus nominal strain curve for the sandwich specimen (core thickness c=25 mm) is given in Fig. 14(*c*), for the case of loading transverse to the roll direction of the faces. The figure includes a simple rule-of-mixtures estimate for the tensile response of the sandwich plate, based on the assumption that the axial strain is uniform across the section. It is evident that the prediction is accurate up to an axial strain of about 0.8%; beyond this strain, unsupported face sheets undergo tensile necking while

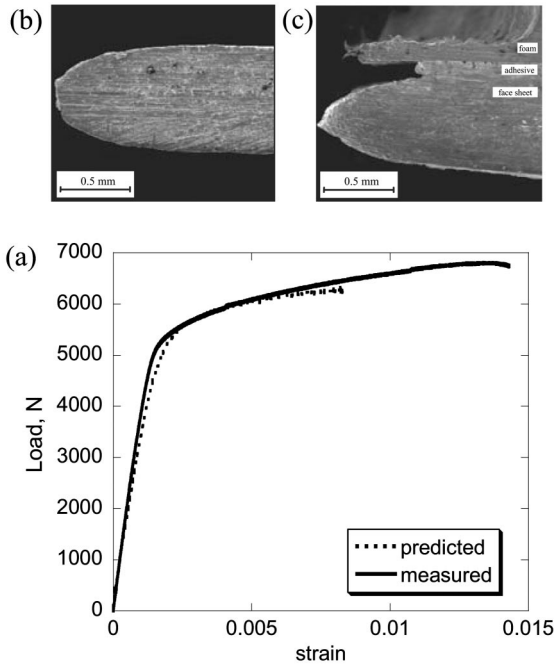

Fig. 14 Scanning electron micrographs of the tensile necks in (*a*) aluminium alloy face sheet with no foam support, and (*b*) aluminium alloy face sheet as part of a sandwich plate. (*c*) Measured tensile load vs strain response for a sandwich dog-bone specimen. The predicted response by an upper bound, rule-of-mixtures calculation is included.

the sandwich specimen remains stable up to a strain of 1.45%. This supports the hypothesis that the foam core stabilises the faces against tensile necking.

The magnitude of the delay in necking is dependent upon ratio of face sheet thickness to core thickness t/c, as shown by the ratio of ductility of sandwich ε_{sw} to that of the faces ε_{fs}, see Fig. 15. It is evident from the figure that this ratio increases with decreasing face sheet thickness and with decreasing ductility of the face sheet. The effect can be large: the measured ductility of the sandwich specimen can be almost doubled by the presence of the foam.

9 Concluding Remarks

This study has focused on the effect of boundary conditions on the flexural response of sandwich beams comprizing aluminium faces and an aluminium foam core. For both simply supported and

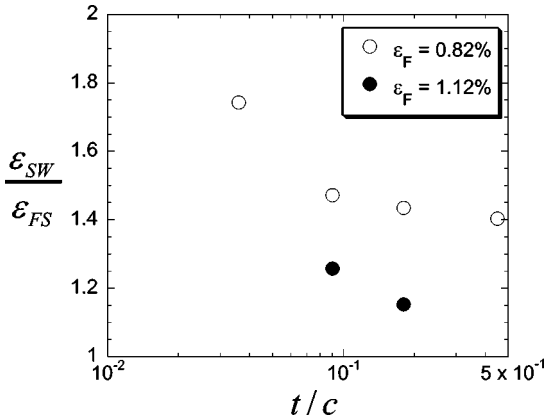

Fig. 15 Sensitivity of tensile ductility of dog-bone sandwich specimens to the ratio of face sheet to core thickness

clamped beams, initial collapse is by core shear, face yield, or by face indentation. Simple limit load calculations and more detailed finite element calculations capture the collapse response except for the case of face sheet indentation; the measured indentation strength is significantly higher than that predicted and it is argued that this is due to the presence of a strengthened boundary layer within the foam adjacent to the face sheets, along the lines discussed by Chen and Fleck [10]. In all clamped beam tests, initial collapse was followed by a stable regime of increasing load with transverse deflection. This regime of membrane stretching begins when the transverse deflection is comparable with the depth of the beam, and ends with tearing of the face sheets. The tensile ductility of the faces is found to be increased by the presence of the foam core—this beneficial effect is due to the stabilization offered by the core to the onset of sheet necking of the faces.

The dominant modes of initial collapse are summarized in a collapse mechanism map, with axes given in terms of the geometry of the beam. The map is useful in the optimizing beam geometry for minimum mass, for any given value of structural load index.

Acknowledgments

This work was supported by the U.S. Office of Naval Research, Contract No. 0014-91-J-1916. The authors are grateful to Dr. V. S. Deshpande and Dr. M. P. Zupan for helpful discussions.

References

[1] Ashby, M. F., Evans, A. G., Fleck, N. A., Gibson L. J., Hutchinson J. W., and Wadley H. N. C., 2000, *Metal Foam: A Design Guide*, Butterworth, Washington, DC.

[2] Evans, A. G., Hutchinson, J. W., Fleck, N. A., Ashby, M. F., and Wadley, H. N. G., 2001, "The Topological Design of Multifunctional Cellular Material," Prog. Mater. Sci., **46**(3–4), pp. 309–327.

[3] Wadley, H. N. G., Fleck, N. A., and Evans, A. G., 2003, "Fabrication and Structural Performance of Periodic Cellular Metal Sandwich Structures," Compos. Sci. Technol. **63**, pp. 2331–2343.

[4] Chen, C., Harte, A.-M., and Fleck, N. A., 2000, "The Plastic Collapse of Sandwich Beams With a Metallic Foam Core," Int. J. Mech. Sci., **43**, pp. 1483–1506.

[5] Bart-Smith, H., Hutchinson, J. W., and Evans, A. G., 2001, "Measurement and Analysis of the Structural Performance of Cellular Metal Sandwich Construction," Int. J. Mech. Sci., **43**, pp. 1945–1963.

[6] Allen, H. G., 1969, *Analysis and Design of Structural Sandwich Panels*, Pergamon Press, NewYork.

[7] Gibson, L. J., and Ashby, M. F., 1997, *Cellular Solids, Structure and Properties*, 2nd. ed., Cambridge University Press, Cambridge, UK.

[8] Deshpande, V. S., and Fleck, N. A., 2000, "Isotropic Constitutive Models for Metallic Foams," J. Mech. Phys. Solids **48**(6–7), pp. 1253–1283.

[9] Chen, C., 1998, "Manual for a UMAT User Subroutine," Cambridge University Engineering Department Report, CUED/C-MICROMECHANICS/TR.4.

[10] Chen, C., and Fleck, N. A., 2002, "Size Effects in the Constrained Deformation of Metallic Foams," J. Mech. Phys. Solids, **50**, pp. 955–977.

[11] Tagarielli, V. L., Fleck, N. A., and Deshpande, V. S., 2003, "Three-Points Bending of Clamped Composite Sandwich Beams," Composites, Part B, **35**, pp. 523–534.